Bioorganic & Medicinal Chemistry Letters 23 (2013) 1720–1726

Contents lists available at SciVerse ScienceDirect

Bioorganic & Medicinal Chemistry Letters

journal homepage: www.elsevier.com/locate/bmcl

Design, synthesis and structure–activity relationship of rhenium 2-arylbenzothiazoles as β-amyloid plaque binding agents

Jinhe Pan [a], Neale S. Mason [b], Manik L. Debnath [c], Chester A. Mathis [b], William E. Klunk [c], Kuo-Shyan Lin [a,*]

[a] Department of Molecular Oncology, BC Cancer Agency, Vancouver, BC, Canada V5Z1L3
[b] Department of Radiology, University of Pittsburgh, Pittsburgh, PA 15213, USA
[c] Department of Psychiatry, University of Pittsburgh, Pittsburgh, PA 15213, USA

ARTICLE INFO

Article history:
Received 18 November 2012
Revised 6 January 2013
Accepted 16 January 2013
Available online 24 January 2013

Keywords:
Technetium-99m
Rhenium
SPECT
PiB
Flutemetamol
β-Amyloid plaques
Alzheimer's disease

ABSTRACT

To continue our efforts toward the development of ^{99m}Tc PiB analogs, we have synthesized 24 neutral and lipophilic Re (as a surrogate of ^{99m}Tc) 2-arylbenzothiazoles, and explored their structure–activity relationship for binding to $A\beta_{1-40}$ fibrils. These Re complexes were designed and synthesized via the integrated approach, so their ^{99m}Tc analogs would have a greater chance of crossing the blood–brain barrier. While the lipophilicities ($\log P_{C18}$ = 1.59–3.53) of these Re 2-arylbenzothiazoles were all within suitable range, their binding affinities (K_i = 30–617 nM) to $A\beta_{1-40}$ fibrils varied widely depending on the selection and integration of the tetradentate chelator into the 2-phenylbenzothiazole pharmacophore. For potential clinical applications, further refinement to obtain Re 2-arylbenzothiazoles with better binding affinities (<10 nM) will likely be needed. The integrated approach reported here to generate compact, neutral and lipophilic Re 2-arylbenzothiazoles could be applied to other potent pharmacophores as well to convert other current Aβ PET tracers to their ^{99m}Tc analogs for more widespread application via the use of SPECT scanners.

Alzheimer's disease (AD) is a progressive and fatal neurodegenerative disorder characterized by irreversible memory impairment, continuous cognitive decline and behavioral disturbances. AD causes about two thirds of dementia in the elderly.[1] It is estimated that by the year of 2050, there will be 13.2 million cases of AD in the US.[2] At present, there is no medical treatment that cures or prevents AD. The production and accumulation of β-amyloid peptides (Aβ) is believed to be pivotal to the pathogenesis and progression of AD,[3] and therefore, research on the treatment of AD has focused on the anti-amyloid therapies.[4] It is well documented that the formation of Aβ plaques precedes the appearance of clinical symptoms.[5] In order to achieve the best therapeutic outcome, it may be necessary to identify potential subjects for therapy before neurons are damaged by Aβ aggregates. Therefore, the development of a noninvasive imaging method capable of quantifying the deposition of Aβ plaques could provide a useful tool for identifying preclinical cases of AD as candidates for early intervention and to follow the effectiveness of anti-amyloid therapy in individual patients.[6]

Toward this end, the development of Aβ plaque-targeting radiotracers for use with positron emission tomography (PET) and single photon emission tomography (SPECT) has been an active research topic in the past two decades.[7,8] PET and SPECT are effective nuclear imaging modalities to detect probes that bind saturable binding sites because their high sensitivity is suitable for extremely low tracer concentrations. Both modalities are now commonly coupled with computed tomography (CT) to generate hybrid images that provide the benefits of both structural and functional/molecular information. Currently, there are several ^{11}C- and ^{18}F-labeled Aβ PET tracers that have been successfully applied in clinical research studies of AD (Fig. 1). Among these imaging agents, 2-(4-[^{11}C]methylaminophenyl)-6-hydroxybenzothiazole (Pittsburgh compound B, PiB)[9] has a high signal-to-noise ratio and has been adopted to perform AD-related research studies worldwide. Unfortunately, due to its short half-life (20 min), the ^{11}C-label on PiB limits its use to major academic PET facilities with on-site cyclotrons and sophisticated radiochemistry laboratories. Promising radiotracers labeled with the longer half-life (110 min) radioisotope ^{18}F have been developed. Among them, florbetapir[10] has recently been approved by the US food and drug administration (FDA) for clinical use for ruling out AD. Manufacturers of other ^{18}F-labeled tracers such as florbetaben,[11] flutemetamol[12] and NAV4694[13] are expected to seek FDA approval in the next few years. These ^{18}F-labeled PET tracers could increase the availability of Aβ imaging to all PET facilities, but this still represents a minority of modern hospitals with PET scanners. Many more hospitals have the capacity to perform SPECT imaging. Aβ imaging agents labeled with SPECT radionuclides, particularly inexpensive and

* Corresponding author. Address: 675 West 10th Avenue, Rm 4-123, Vancouver, BC, Canada V5Z1L3. Tel.: +1 604 675 8208; fax: +1 604 675 8218.
E-mail address: klin@bccrc.ca (K.-S. Lin).

0960-894X/$ - see front matter © 2013 Elsevier Ltd. All rights reserved.
http://dx.doi.org/10.1016/j.bmcl.2013.01.068

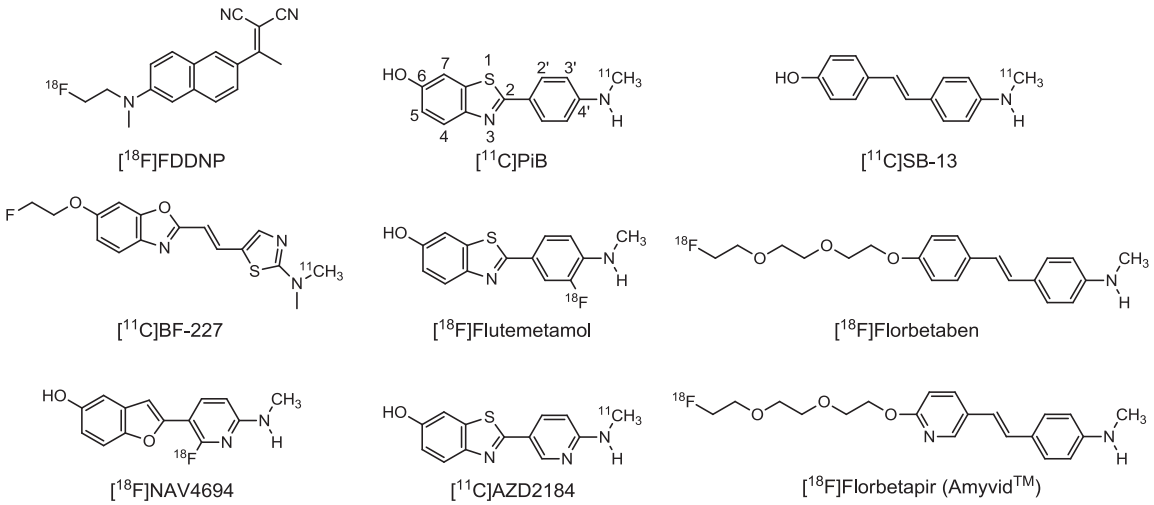

Figure 1. PET Aβ imaging agents currently under clinical evaluation.

readily available ^{99m}Tc will have more widespread clinical applicability especially in developing countries.

With the success in the development of the 2-arylbenzothiazole (2-ABT) based PET radiotracers, PiB and flutemetamol, we were also interested in the development of ^{99m}Tc-labeled 2-ABTs for more widespread application using SPECT scanners. In contrast to most attempts by other investigators on the development of ^{99m}Tc-labeled 2-ABTs using the pendant approach,[14–16] we have previously demonstrated the feasibility of design and synthesis of three neutral and lipophilic Re (as a surrogate of ^{99m}Tc) 2-ABTs (compounds# **6**, **12** and **21** in Table 1) with moderate Aβ binding affinity (30–87 nM) using the integrated approach to minimize their overall molecular weight (<550 Da).[17] Compound **6** was prepared using a thiol-triamine SN_3 tetradentate chelator (Scheme 1A), while semi-rigid thiol-diamine-phenol (SN_2O) and thiol-diamine-thiol (SN_2S) chelators (Scheme 1B, X = O and S) were used for the preparation of **12** and **21**, respectively. Besides the SN_3, SN_2O and SN_2S chelators, the semi-rigid thiol-diamine-thioether (SN_2Sether)[18] chelator is also commonly used for the design and synthesis of neutral and lipophilic Tc/Re complexes. While SN_3, SN_2X, SN_2Sether chelators all form stable Tc/Re complexes, the preparation of Tc/Re 2-ABTs by the use of different tetradentate chelators or the same chelator integrated at different positions of the pharmacophore might generate Tc/Re 2-ABTs with different binding affinity, lipophilicity and in vivo pharmacokinetics. The aim of this present work was to systematically explore the potential of utilizing SN_3, SN_2X, and SN_2Sether chelators to generate compact, neutral, and lipophilic Re 2-ABTs, and to investigate the structure–activity relationship for their lipophilicity and binding affinity to aggregated Aβ.

As shown in Table 1, besides **6**, **12** and **21** that were reported earlier, we synthesized an additional 21 Re 2-ABTs with chelators integrated at different positions of 2-ABT pharmacophore for comparison. Our previous results[19,20] indicated that substitution on the 2-ABT pharmacophore with an electron-donating group or a halogen significantly increases the binding affinity. For example, the K_i for an amino, *N*-methylamino, *N*,*N*-dimethylamino, fluoro, bromo, or iodo substitution at the 4′-position of 2-ABT were 37.0, 11.0, 4.0, 43.8, 8.8, and 2.6 nM, respectively. The definition of substitution positions is depicted on the structure of PiB shown in Figure 1. The integration of a tetradentate chelator into the benzothiazole ring provides an electron-donating group at the 6-position (compounds **1**–**3**), whereas the integration of a tetradentate chelator into the phenyl ring provides an electron-donating group at the 4′-position (compounds **4**–**6**) or both the 3′- and 4′-position (compounds **7**–**24**). To further enhance their binding affinity, we also synthesized analogs with a fluoro or methoxy substitution at the 6-position when a tetradentate chelator is integrated into the phenyl ring, or at the 4′-position when a tetradentate chelator is integrated into the benzothiazole ring. The choice of the small halogen fluorine and a methoxy group is to limit the overall size increase. In addition, substitution with an aromatic fluoro or methoxy group will not significantly change the overall lipophilicity.

The synthetic steps for the preparation of Re 2-ABT **1**–**24** are depicted in Schemes 2–9. The SN_3 chelator used for the preparation of **1**–**6** (Schemes 2 and 3) was modified from the thiol-triamide.[21,22] chelator as shown in Scheme 1A. Complexation of the original thiol-triamide chelator with $[Tc(V)O]^{3+}$ or $[Re(V)O]^{3+}$ led to metal complexes with one negative charge due to the loss of four protons from three amide N–H groups and one thiol S–H group. It is well documented that charged Tc complexes do not cross the blood–brain barrier (BBB). In addition, Tc complexes derived from tetradentate chelators containing amide groups (such as mono-amide-monoamine-dithiol, MAMA) showed less brain uptake when compared to those derived from their corresponding amino chelators (such as diaminedithiol, DADT).[23,24] Therefore, we modified the original thiol-triamide chelator by replacing the three amide groups with three amino groups. In order to obtain neutral Tc/Re complexes, we also added one small methyl group to one of the aliphatic amino groups. After such modification (see Scheme 1A), all three protons were lost after complexation with $[Re(V)O]^{3+}$, and the overall charge of 2-ABT **1**–**5** was balanced, which is in agreement with our previously reported results from the synthesis of **6**.[17]

Re 2-ABTs **7**–**9** (Scheme 4), **10**–**15** (Schemes 5 and 6), and **16**–**21** (Schemes 7 and 8) were synthesized using modified semi-rigid SN_2X chelators (Scheme 1B, X = NH, O, and S, respectively) integrated into the 3′- and 4′-position of phenyl ring. This design was to further reduce their overall molecular weight to 500 daltons or less as suggested by the rule of five,[25] and in hopes that their corresponding ^{99m}Tc analogs would show rapid and high brain entry. These semi-rigid SN_2X chelating systems were modified from previously reported thiol-diamide-X systems (X = NX, O and S).[26] As shown in Scheme 1B, the complexation of $[Re(V)O]^{3+}$ with thiol-diamide-X chelating systems led to Re complexes with one negative charge. Similar to our modification to the thiol-triamide chelator shown in Scheme 1A, we also replaced the two amide groups with two amino groups in order to produce neutral Re complexes and increase brain uptake of

Table 1
Properties of Re 2-phenylbenzothiazoles including molecular weight (MW), binding affinity (K_i) to $A\beta_{1-40}$, and lipophilicity ($\log P_{C18}$)

Compd #	Structure	R	MW	K_i (nM)	$\log p_{c18}$
1	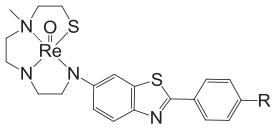	H	586 (498[a])	556	2.54
2		F	604 (516[a])	617	2.67
3		OMe	616 (528[a])	85	2.37
4	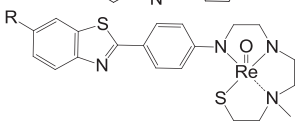	H	586 (498[a])	378	2.65
5		F	604 (516[a])	118	2.84
6		OMe	616 (528[a])	87	2.52
7	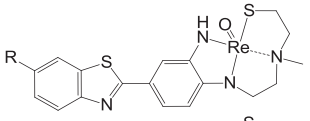	H	558 (470[a])	90	2.33
8		F	576 (488[a])	113	2.50
9		OMe	588 (500[a])	61	2.21
10	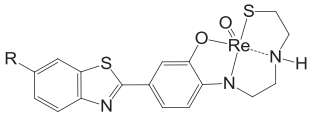	H	545 (457[a])	109	1.70
11		F	563 (475[a])	64	1.90
12		OMe	575 (487[a])	30	1.65
13	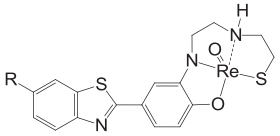	H	545 (457[a])	280	1.68
14		F	563 (475[a])	226	1.87
15		OMe	575 (487[a])	140	1.59
16	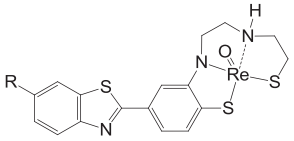	H	561 (473[a])	264	2.49
17		F	579 (491[a])	93	2.65
18		OMe	591 (503[a])	132	2.45
19	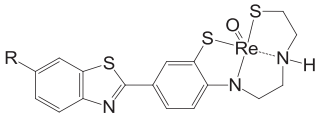	H	561 (473[a])	38	2.41
20		F	579 (491[a])	31	2.60
21		OMe	591 (503[a])	43	2.30
22	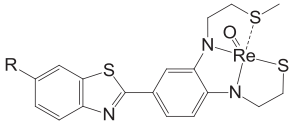	H	575 (487[a])	200	3.35
23		F	593 (505[a])	148	3.53
24		OMe	605 (517[a])	178	3.25

[a] Molecular weight of their corresponding Tc analogs.

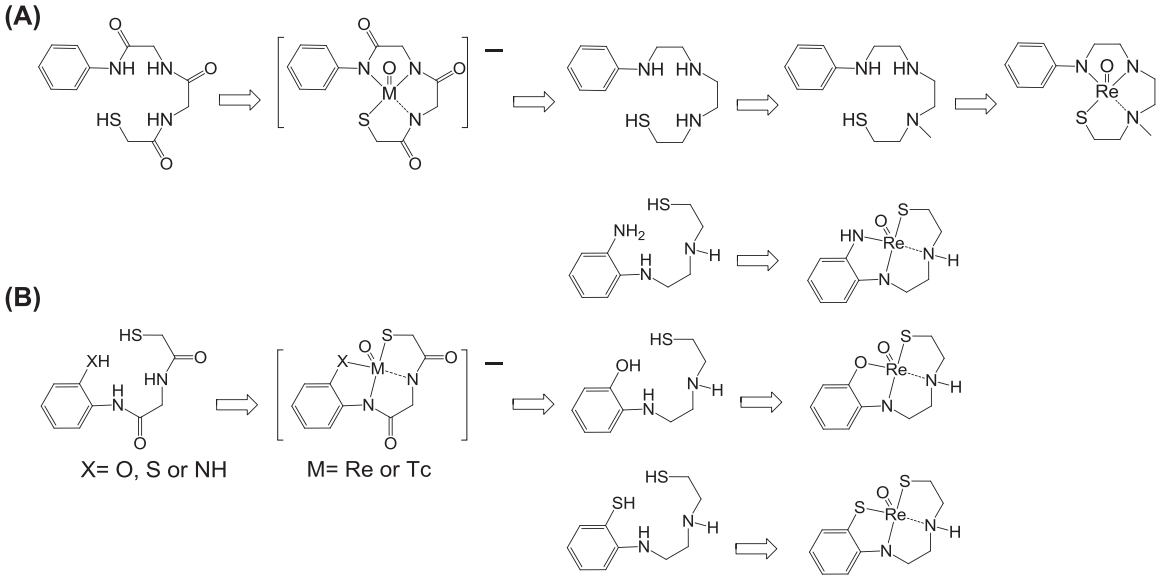

Scheme 1. Design and synthesis of neutral Re 2-arylbenzothiazoles by modification of reported (A) SN_3 chelating system, and (B) SN_2X chelating system.

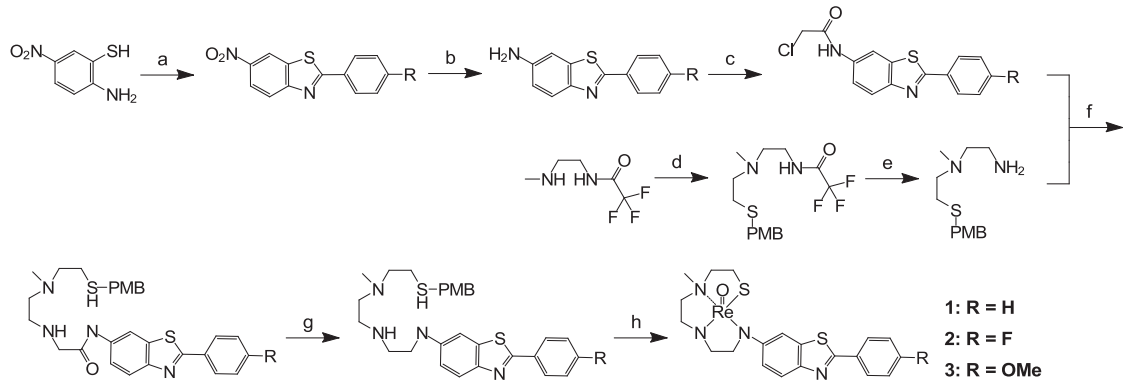

Scheme 2. Synthesis of **1–3**. Reagents and conditions: (a) 4-substituted benzoyl chloride, DMF, 140 °C, 18 h, 57–90%; (b) $SnCl_2$, EtOH, 3 h, reflux, 73–91%; (c) 2-chloroacetyl chloride, K_2CO_3, THF, 18 h, rt, 94–99%; (d) 2-(4-methoxybenzylthio)ethyl bromide, CH_2Cl_2, 18 h, reflux, 81%; (e) NaOH, H_2O, MeOH, 4 h, rt, 92%; (f) KI, K_2CO_3, CH_3CN, 14 h, reflux, 35–68%; (g) LAH, THF, 18 h, rt, 38–80%; (h) (i) TFA, anisole, rt, 1 h; (ii) $Hg(OAc)_2$ 0 °C, 1 h; (iii) H_2S, EtOH; (iv) $ReO(PPh_3)_2Cl_3$, NaOAc, MeOH, 18 h, 75 °C, 16–29%.

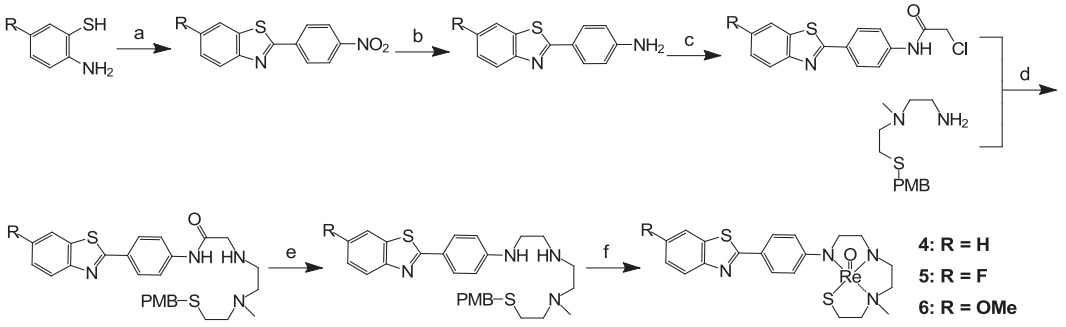

Scheme 3. Synthesis of **4–6**. Reagents and conditions: (a) 4-nitrobenzoyl chloride, DMF, 140 °C, 18 h, 38–80%; (b) $SnCl_2$, EtOH, 3 h, reflux, 88–100%; (c) 2-chloroacetyl chloride, K_2CO_3, THF, 18 h, rt, 92–96%; (d) KI, K_2CO_3, CH_3CN, 18 h, reflux, 63–88%; (e) LAH, THF, 18 h, rt, 42–58%; (f) (i) TFA, anisole, rt, 1 h; (ii) $Hg(OAc)_2$ 0 °C, 1 h; (iii) H_2S, EtOH; (iv) $ReO(PPh_3)_2Cl_3$, NaOAc, MeOH, 18 h, 75 °C, 19–41%.

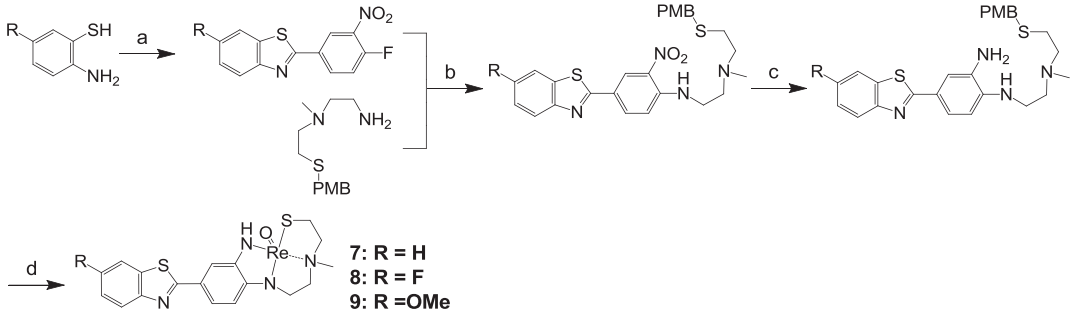

Scheme 4. Synthesis of **7–9**. Reagents and conditions: (a) 4-fluoro-3-nitrobenzoyl chloride, DMF, 140 °C, 18 h, 58–92%; (b) K_2CO_3, DMF, 100 °C, 18 h, 27–81%; (c) $SnCl_2$, EtOH, 3 h, reflux, 10–81%; (d) (i) TFA, anisole, rt, 1 h; (ii) $Hg(OAc)_2$ 0 °C, 1 h; (iii) H_2S, EtOH; (iv) $ReO(PPh_3)_2Cl_3$, NaOAc, MeOH, 18 h, 75 °C, 10–39%.

their ^{99m}Tc analogs. As expected, after complexation with $[Re(V)O]^{3+}$, only three protons were lost. The aliphatic amino N–H group that has relatively higher pK_a value was not de-protonated after Re complexation reaction, and therefore, the overall charge was balanced. These results were consistent with our previously reported results for the synthesis of **12** and **21**.[17]

Syntheses of **22–24** are shown in Scheme 9 using the previously reported semi-rigid SN_2Sether chelator.[18] The methyl thioether group was chosen to keep the overall molecular weight at minimum. After complexation with $[Re(V)O]^{3+}$, as expected, neutral Re 2-ABT **22–24** were obtained resulting from the loss of three protons (two aromatic N–H and one thiol S–H groups). The final step in the preparation of Re 2-ABT **1–24** involved a two-stage reaction, deprotection of *p*-methoxybenzyl (PMB)/methoxymethyl (MOM) protecting groups to restore the chelating core followed by Re complexation reaction using $Re(V)O(PPh_3)_2Cl_3$.[27] In spite of potential existence of *cis*- and *anti*-isomers, similar to our previous results for the syntheses of **6**, **12** and **21**,[17] only one single isomer was isolated for each of these additional 21 Re 2-ABTs reported here, and their identities were confirmed by NMR spectroscopy.[28]

Re 2-ABT **1–24** are moderately lipophilic with logP_{C18} (P_{C18}: estimation of P_{oct} by a reverse-phase HPLC method[19]) in the range of 1.59–3.53 (Table 1). Among them, **10–15** derived from the SN_2O chelator displayed the lowest lipophilicity (logP_{C18} = 1.59–1.90), whereas **22–24** derived from the SN_2Sether chelator had the highest lipophilicity (logP_{C18} = 3.25–3.53). Replacing the phenol of the SN_2O chelator in **10–15** with a thiol resulted in Re SN_2S derivatives **16–21** with an average increase of 0.75 in their logP_{C18} values (**10–12** vs **19–21**; **13–15** vs **16–18**). The Re 2-ABTs derived from the same tetradentate chelator (SN_2O or SN_2S) but with different

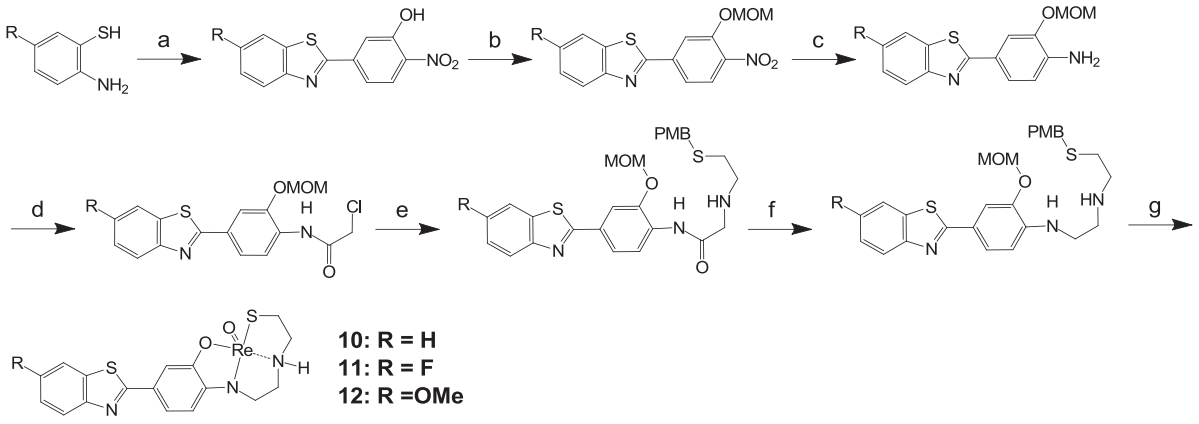

Scheme 5. Synthesis of **10**–**12**. Reagents and conditions: (a) 3-hydroxy-4-nitro benzaldehyde, DMSO, 125 °C, 18 h, 15–65%; (b) MOMCl, DIPEA, THF, 18 h, reflux, 51–71% (c) $NaBH_4$, $Cu(OAc)_2$, EtOH, rt, 18 h, 96–100%; (d) 2-chloroacetyl chloride, K_2CO_3, THF, 18 h, rt, 64–82%; (e) 2-(4-methoxybenzylthio)ethylamine, KI, K_2CO_3, CH_3CN, 18 h, reflux, 80–98%; (f) LAH, THF, 18 h, rt, 43–45%; (g) (i) TFA, anisole, rt, 1 h; (ii) $Hg(OAc)_2$ 0 °C, 1 h; (iii) H_2S, EtOH; (iv) $ReO(PPh_3)_2Cl_3$, NaOAc, MeOH, 18 h, 75 °C, 17–49%.

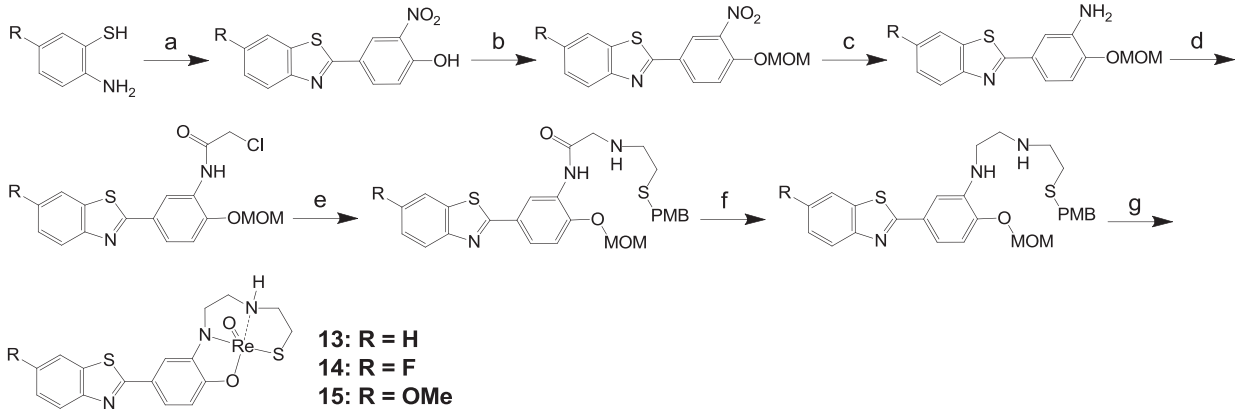

Scheme 6. Synthesis of **13**–**15**. Reagents and conditions: (a) 4-hydroxy-3-nitro benzaldehyde, DMSO, 125 °C, 18 h, 28-35%; (b) MOMCl, DIPEA, THF, reflux, 18 h, 98–99%; (c) $NaBH_4$, $Cu(OAc)_2$, EtOH, rt, 18 h, 92–97%; (d) 2-chloroacetyl chloride, K_2CO_3, THF, 18 h, rt, 79–91%; (e) 2-(4-methoxybenzylthio)ethylamine, KI, K_2CO_3, CH_3CN, 18 h, reflux, 40–96%; (f) LAH, THF, 17 h, rt, 43–59%; (g) (i) TFA, anisole, rt, 1 h; (ii) $Hg(OAc)_2$ 0 °C, 1 h; (iii) H_2S, EtOH; (iv) $ReO(PPh_3)_2Cl_3$, NaOAc, MeOH, 18 h, 75 °C, 20–41%.

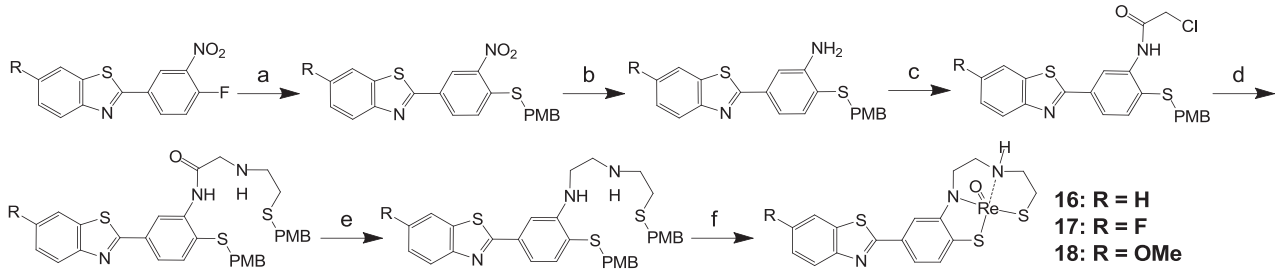

Scheme 7. Synthesis of **16**–**18**. Reagents and conditions: (a) 4-methoxy-α-toluenethiol, K_2CO_3, DMF, 18 h, 100 °C, 35–77%; (b) $SnCl_2$, THF, EtOH, 3 h, reflux, 57–95%; (c) 2-chloroacetyl chloride, K_2CO_3, THF, 18 h, rt, 90–93%; (d) 2-(4-methoxybenzylthio)ethylamine, KI, K_2CO_3, CH_3CN, 18 h, reflux, 43–84%; (e) LAH, THF, 18 h, rt, 24–53%; (f) (i) TFA, anisole, rt, 1 h; (ii) $Hg(OAc)_2$ 0 °C, 1 h; (iii) H_2S, EtOH; (iv) $ReO(PPh_3)_2Cl_3$, NaOAc, MeOH, 18 h, 75 °C, 25–36%.

integration patterns into the phenyl ring (the amino group substituted at the 3′- or 4′-position) had similar lipophilicity (**10**–**12** vs **13**–**15**; **16**–**18** vs **19**–**21**). Compared with **1**–**6** derived from the SN_3 chelating system with only one lateral amino group of the chelator integrated into the 2-ABT backbone, **7**–**9** derived from the semi-rigid SN_3 chelator with two amino groups integrated into the phenyl ring had lower lipophilicity due to the presence of an amino N–H proton at the 3′-position and one less ethylene moiety in the overall structure. If comparing the Re 2-ABTs with the same tetradentate chelator but with different substitution (H, F and OMe) at the 6- or 4′-position, the methoxy-substituted 2-ABTs had the lowest $\log P_{C18}$ values with an average of 0.10 and 0.25 lower than those of their respective un-substituted and fluoro-substituted Re 2-ABTs.

Re 2-ABTs **1**–**24** bind $A\beta_{1-40}$ fibrils with moderate to poor affinity (K_i = 30–617 nM, Table 1) as determined by previously published in vitro competition binding assays[19,29] using [^{3}H]BTA-1 as the radioactive control compound. In general, compared to the un-substituted Re 2-ABTs, substitution with a fluoro or a methoxy group at the 6- or 4′-position enhanced their binding affinity to $A\beta_{1-40}$ fibrils. The integration of an SN_3 chelator into the phenyl ring (in **4**–**6**) rather than the benzothiazole ring (in **1**–**3**) resulted in Re

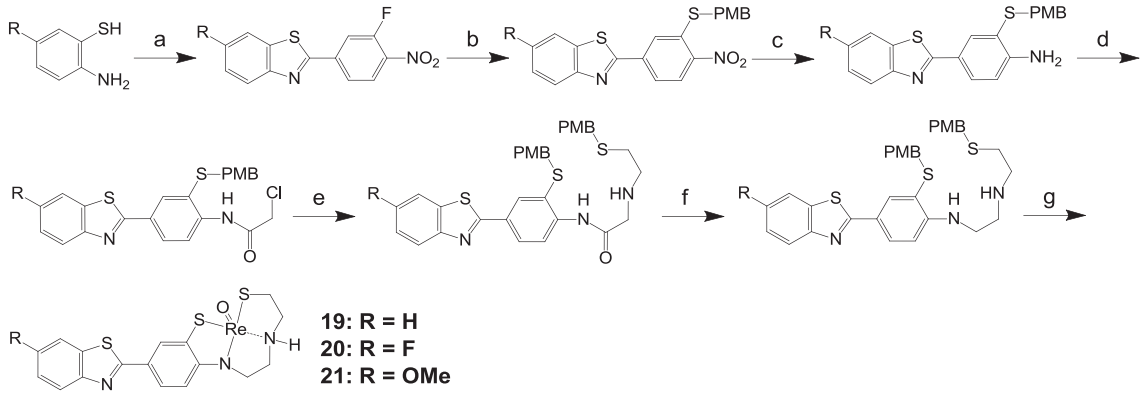

Scheme 8. Synthesis of **19–21**. Reagents and conditions: (a) 3-fluoro-4-nitrobenzoyl chloride, DMF, 140 °C, 18 h, 73–99%; (b) 4-methoxy-α-toluenethiol, K_2CO_3, DMF, 18 h, 95 °C, 55–96%; (c) $SnCl_2$, THF, EtOH, 3 h, reflux, 67–79%; (d) 2-chloroacetyl chloride, K_2CO_3, THF, 18 h, rt, 81–98%; (e) 2-(4-methoxybenzylthio)ethylamine, KI, K_2CO_3, CH_3CN, 18 h, reflux, 75–93%; (f) LAH, THF, 18 h, rt, 56–81%; (g) (i) TFA, anisole, rt, 1 h; (ii) $Hg(OAc)_2$ 0 °C, 1 h; (iii) H_2S, EtOH; (iv) $ReO(PPh_3)_2Cl_3$, NaOAc, MeOH, 18 h, 75 °C, 12–23%.

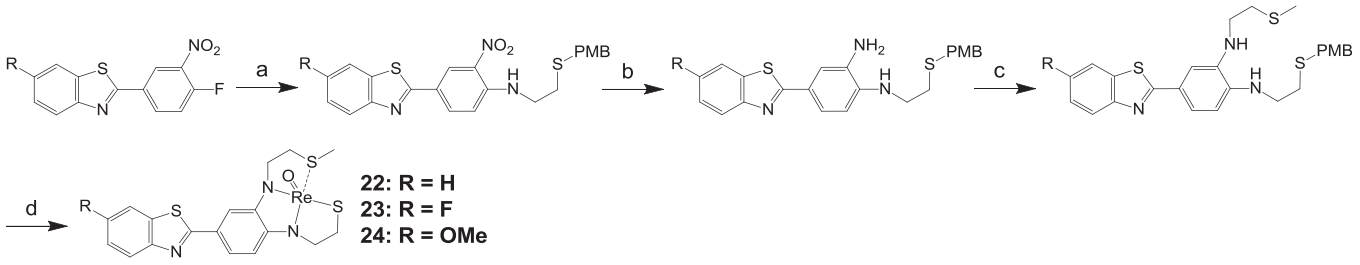

Scheme 9. Synthesis of **22–24**. Reagents and conditions: (a) 2-(4-methoxybenzylthio)ethylamine, K_2CO_3, DMF, 100 °C, 18 h, 41–96%; (2) $SnCl_2$, THF, EtOH, 3 h, reflux, 55–98%; (c) 2-chloroethyl methyl sulfide, KI, K_2CO_3, CH_3CN, 18 h, reflux, 40–64%; (d) (i) TFA, anisole, rt, 1 h; (ii) $Hg(OAc)_2$ 0 °C, 1 h; (iii) H_2S, EtOH; (iv) $ReO(PPh_3)_2Cl_3$, NaOAc, MeOH, 18 h, 75 °C, 25–26%.

2-ABTs with better binding affinities. Replacing the free rotating Re-SN_3 complex in **4–6** with a semi-rigid Re-SN_3 complex in **7–9** further enhance the binding affinity. As discussed above, different integration patterns of the same tetradentate chelator (SN_2O or SN_2S) had little effects on the overall lipophilicity of the resulted Re 2-ABTs (**10–12** vs **13–15**; **16–18** vs **19–21**). However, the binding affinities of these 2-ABTs were strongly influenced by the integration patterns of the tetradentate chelator. When comparing the 2-ABTs **10–15** with the semi-rigid SN_2O chelator, **10–12** (K_i = 30–109 nM) with an amino group of the chelator substituted at the 4′-position had 2.6- to 4.7-fold better binding affinity than their corresponding analogs **13–15** (K_i = 140–280 nM) with the amino group substituted at the 3′-position. Similar results were obtained when comparing the binding affinity of Re 2-ABTs **16–21** with the semi-rigid SN_2S chelator. The binding affinities of **19–21** (K_i = 31–43 nM) with an amino group of the SN_2S chelator substituted at the 4′-position were 3.1- to 6.9-fold better than those of their corresponding analogs **16–18** (K_i = 93–264 nM) with the amino group substituted at the 3′-position. These results are in agreement with the fact that most of the promising PET tracers derived from the 2-ABT pharmacophore including [^{11}C]PiB, [^{11}C]AZD2184, and [^{18}F]flutemetamol (see Fig. 1) have an amino group substituted at the 4′-position.

In summary, we have synthesized twenty-four neutral and compact Re 2-ABTs, and measured their lipophilicity and binding affinity to aggregated Aβ. These Re 2-ABTs were designed and prepared via the integrated approach, so their ^{99m}Tc analogs would have a greater chance of crossing the BBB, and bind to Aβ plaques deposited in the brain parenchyma. While the lipophilicities of these 2-ABTs were within suitable range ($\log P_{C18}$ = 1–4), their binding affinities (K_i = 30–617 nM) to $A\beta_{1-40}$ fibrils varied widely depending on the selection of the chelators, and the ways the chelators were integrated into the 2-ABT pharmacophore. Based on the binding affinity data, we have identified two promising semi-rigid chelators, SN_2O and SN_2S. The Re 2-ABTs **12** and **20** derived from the SN_2O and SN_2S chelators, respectively, had fairly good binding affinity ($K_i \sim 30$ nM) to $A\beta_{1-40}$ fibrils. However, before translation into their ^{99m}Tc analogs and for potential clinical application, further modification to obtain Re 2-ABTs with even better binding affinity will likely be needed since most of the clinical Aβ imaging agents have binding affinities less than 10 nM. This might be achievable by optimizing the substitution at the 6-position of the 2-ABT pharmacophore with other potent electron-donating groups, and/or by the 3D-QSAR analysis as recently reported by Kim et al.[30] and Yang et al.[31] The integrated approach reported here to generate compact, neutral and lipophilic Re 2-arylbenzothiazoles could be applied to generate Re complexes of other potent pharmacophores, including stilbene and benzoxazole. Once potent Re complexes are obtained, their ^{99m}Tc analogs will have great potential to extend current Aβ imaging practices from PET to SPECT.

Acknowledgement

This work was supported by the US National Institutes of Health (R21EB009497).

References and notes

1. Nussbaum, R. L.; Ellis, C. E. *N. Engl. J. Med.* **2003**, *348*, 1356.
2. Hebert, L. E.; Scherr, P. A.; Bienias, J. L.; Bennett, D. A.; Evans, D. A. *Arch. Neurol.* **2003**, *60*, 1119.
3. Hardy, J.; Selkoe, D. J. *Science* **2002**, *297*, 353.
4. Pangalos, M. N.; Jacobsen, S. J.; Reinhart, P. H. *Biochem. Soc. Trans.* **2005**, *33*, 553.

5. Pike, K. E.; Savage, G.; Villemagne, V. L.; Ng, S.; Moss, S. A.; Maruff, P.; Mathis, C. A.; Klunk, W. E.; Masters, C. L.; Rowe, C. C. *Brain* **2007**, *130*, 2837.
6. Mathis, C. A.; Lopresti, B. J.; Klunk, W. E. *Nucl. Med. Biol.* **2007**, *34*, 809.
7. Mathis, C. A.; Wang, Y.; Klunk, W. E. *Curr. Pharm. Des.* **2004**, *10*, 1469.
8. Mori, T.; Maeda, J.; Shimada, H.; Higuchi, M.; Shinotoh, H.; Ueno, S.; Suhara, T. *Psychogeriatrics* **2012**, *12*, 106.
9. Klunk, W. E.; Engler, H.; Nordberg, A.; Wang, Y. M.; Blomqvist, G.; Holt, D. P.; Bergstrom, M.; Savitcheva, I.; Huang, G. F.; Estrada, S.; Ausen, B.; Debnath, M. L.; Barletta, J.; Price, J. C.; Sandell, J.; Lopresti, B. J.; Wall, A.; Koivisto, P.; Antoni, G.; Mathis, C. A.; Langstrom, B. *Ann. Neurol.* **2004**, *55*, 306.
10. Clark, C. M.; Schneider, J. A.; Bedell, B. J.; Beach, T. G.; Bilker, W. B.; Mintun, M. A.; Pontecorvo, M. J.; Hefti, F.; Carpenter, A. P.; Flitter, M. L.; Krautkramer, M. J.; Kung, H. F.; Coleman, R. E.; Doraiswamy, P. M.; Fleisher, A. S.; Sabbagh, M. N.; Sadowsky, C. H.; Reiman, P. E. M.; Zehntner, S. P.; Skovronsky, D. M. *JAMA, J. Am. Med. Assoc.* **2011**, *305*, 275.
11. Rowe, C. C.; Ackerman, U.; Browne, W.; Mulligan, R.; Pike, K. L.; O'Keefe, G.; Tochon-Danguy, H.; Chan, G.; Berlangieri, S. U.; Jones, G.; Dickinson-Rowe, K. L.; Kung, H. F.; Zhang, W.; Kung, M. P.; Skovronsky, D.; Dyrks, T.; Hall, G.; Krause, S.; Friebe, M.; Lehman, L.; Lindemann, S.; Dinkelborg, L. M.; Masters, C. L.; Villemagne, V. L. *Lancet Neurol.* **2008**, *7*, 129.
12. Nelissen, N.; Van Laere, K.; Thurfjell, L.; Owenius, R.; Vandenbulcke, M.; Koole, M.; Bormans, G.; Brooks, D. J.; Vandenberghe, R. *J. Nucl. Med.* **2009**, *50*, 1251.
13. Cselenyi, Z.; Jonhagen, M. E.; Forsberg, A.; Halldin, C.; Julin, P.; Schou, M.; Johnstrom, P.; Varnas, K.; Svensson, S.; Farde, L. *J. Nucl. Med.* **2012**, *53*, 415.
14. Serdons, K.; Vanderghinste, D.; Van Eeckhoudt, M.; Cleynhens, J.; de Groot, T.; Bormans, G.; Verbruggena, A. *J. Labelled Compd. Radiopharm.* **2009**, *52*, 227.
15. Chen, X.; Yu, P.; Zhang, L.; Liu, B. *Bioorg. Med. Chem. Lett.* **2008**, *18*, 1442.
16. Serdons, K.; Verduyckt, T.; Cleynhens, J.; Terwinghe, C.; Mortelmans, L.; Bormansa, G.; Verbruggen, A. *Bioorg. Med. Chem. Lett.* **2007**, *17*, 6086.
17. Lin, K. S.; Debnath, M. L.; Mathis, C. A.; Klunk, W. E. *Bioorg. Med. Chem. Lett.* **2009**, *19*, 2258.
18. McBride, B. J.; Baldwin, R. M.; Kerr, J. M.; Wu, J. L.; Schultze, L. M.; Salazar, N. E.; Chinitz, J. M.; Byrne, E. F. *J. Med. Chem.* **1993**, *36*, 81.
19. Mathis, C. A.; Wang, Y. M.; Holt, D. P.; Huang, G. F.; Debnath, M. L.; Klunk, W. E. *J. Med. Chem.* **2003**, *46*, 2740.
20. KlunK, W. E.; Mathis, C. A. U.S. Patent 0142269A1, 2009.
21. Eisenhut, M.; Mohammed, A.; Mier, W.; Schoensiegel, F.; Friebe, M.; Mahmood, A.; Jones, A. G.; Haberkorn, U. *J. Med. Chem.* **2002**, *45*, 5802.
22. Hansen, L.; Cini, R.; Taylor, A., Jr.; Marzilli, L. G. *Inorg. Chem.* **1992**, *31*, 2801.
23. Zhuang, Z. P.; Kung, M. P.; Hou, C.; Ploessl, K.; Kung, H. F. *Nucl. Med. Biol.* **2005**, *32*, 171.
24. Oya, S.; Plossl, K.; Kung, M. P.; Stevenson, D. A.; Kung, H. F. *Nucl. Med. Biol.* **1998**, *25*, 135.
25. Lipinski, C. A.; Lombardo, F.; Dominy, B. W.; Feeney, P. J. *Adv. Drug Delivery Rev.* **1995**, *23*, 3.
26. Le Gal, J.; Tisato, F.; Bandoli, G.; Gressier, M.; Jaud, J.; Michaud, S.; Dartiguenave, M.; Benoist, E. *Dalton Trans.* **2005**, *23*, 3800.
27. *General procedures for the synthesis of Re complexes* ***1–24****:* A solution of the respective PMB/MOM-protected precursor (0.2 mmol) in trifluoroacetic acid (5 mL) and anisole (0.2 mL) was stirred at room temperature for 1 h, and then cooled in ice/water bath. $Hg(OAc)_2$ (0.48 mmol for the preparation of **16–21**, and 0.24 mmol for the preparation of other Re complexes) was added, and the resulting solution was stirred at 0 °C for another 1 h. After removing volatile trifluoroacetic acid under reduced pressure, the residue was washed with diethyl ether (20 mL), and then dissolved in ethanol (15 mL). To this solution was bubbled in hydrogen sulfide for 10 min, and the resulting black precipitate was removed by filtration through celite. The filtrate was concentrated under reduced pressure. $ReO(PPh_3)_2Cl_3$ (208 mg, 0.25 mmol) and NaOAc methanolic solution (1.0 M, 20 mL) were added to the residue, and the resulting solution was heated at 75 °C for 18 h. After cooling to room temperature, the solution was diluted with water (50 mL), and extracted with chloroform (50 mL). The organic phase was dried over anhydrous magnesium sulfate and concentrated under reduced pressure. The crude product was purified by chromatography on silica gel eluting with 10:90 methanol/ethyl acetate to give the expected product in 10–49% yields.
28. *NMR spectra were recorded using a Bruker Avance 400inv NMR spectrometer.* Chemical shifts (δ) are reported in parts per million (ppm). Compound **1** (DMSO-d_6): 2.04–2.16 (m, 1H), 2.71–2.79 (m, 1H), 3.19 (s, 3H), 3.21–3.27 (m, 2H), 3.39–3.45 (m, 1H), 3.49–3.57 (m, 1H), 3.61–3.70 (m, 1H), 3.83–3.90 (m, 1H), 3.84 (s, 3H), 3.91–3.40 (m, 2H), 3.66–4.73 (m, 1H), 7.36 (dd, J = 8.8, 2.4 Hz, 1H), 7.52–7.64 (m, 3H), 7.70 (d, J = 2.4 Hz, 1H), 7.81 (d, J = 8.8 Hz, 1H), 8.02 (dd, J = 7.8, 2.0 Hz, 2H); Compound **2** (DMSO-d_6): 2.06–2.16 (m, 1H), 2.71–2.79 (m, 1H), 3.19 (s, 3H), 3.21–3.27 (m, 2H), 3.39–3.46 (m, 1H), 3.49–3.58 (m, 1H), 3.62–3.71 (m, 1H), 3.83–3.90 (m, 1H), 3.91–3.40 (m, 2H), 3.66–4.73 (m, 1H), 7.33–7.42 (m, 3H), 7.73 (d, J = 2.0 Hz, 1H), 7.81 (d, J = 8.8 Hz, 1H), 8.04–8.09 (m, 2H); Compound **3** (DMSO-d_6): 2.06–2.16 (m, 1H), 2.71–2.79 (m, 1H), 3.19 (s, 3H), 3.21–3.29 (m, 2H), 3.39–3.46 (m, 1H), 3.50–3.59 (m, 1H), 3.62–3.70 (m, 1H), 3.83–3.90 (m, 1H), 3.84 (s, 3H), 3.91–3.40 (m, 2H), 3.66–4.73 (m, 1H), 7.10 (d, J = 8.8 Hz, 2H), 7.32 (dd, J = 8.8, 2.4 Hz, 1H), 7.67 (d, J = 2.4 Hz, 1H), 7.76 (d, J = 8.8 Hz, 1H), 7.96 (d, J = 8.8 Hz, 2H); Compound **4** (DMSO-d_6): 2.13–2.20 (m, 1H), 2.53–2.58 (m, 1H), 2.75–2.79 (m, 1H), 3.20 (s, 3H), 3.22–3.40 (m, 2H), 3.43–3.50 (m, 2H), 3.64–3.71 (m, 1H), 3.84–3.90 (m, 2H), 3.94–3.99 (m, 1H), 4.59–4.64 (m, 1H), 7.24 (d, J = 8.8 Hz, 2H), 7.36–7.40 (m, 1H), 7.47–7.51 (m, 1H), 7.79 (d, J = 8.8 Hz, 2H), 7.96 (d, J = 8.1 Hz, 1H), 8.70 (d, J = 7.9 Hz, 1H); Compound **5** (DMSO-d_6): 2.13–2.20 (m, 1H), 2.53–2.58 (m, 1H), 2.75–2.79 (m, 1H), 3.20 (s, 3H), 3.22–3.40 (m, 2H), 3.43–3.50 (m, 2H), 3.64–3.70 (m, 1H), 3.80–3.91 (m, 2H), 3.93–3.99 (m, 1H), 4.60–4.64 (m, 1H), 7.24 (d, J = 8.9 Hz, 2H), 7.32–7.38 (m, 1H), 7.87 (d, J = 8.8 Hz, 2H), 7.95–8.01 (m, 2H); Compound **7** (DMSO-d_6): 2.17–2.25 (m, 1H), 3.07–3.23 (m, 3H), 3.30 (s, 3H), 3.74–3.79 (m, 1H), 4.06–4.11 (m, 1H), 4.62–4.69 (m, 1H), 6.88 (d, J = 8.1 Hz, 1H), 7.34–7.38 (m, 2H), 7.46–7.50 (m, 1H), 7.58 (d, J = 1.8 Hz, 1H), 7.95 (d, J = 7.9 Hz, 1H), 8.05 (d, J = 7.5 Hz, 1H), 11.3 (s, 1H); Compound **8** (DMSO-d_6): 2.16–2.25 (m, 1H), 3.05–3.23 (m, 3H), 3.29 (s, 3H), 3.73–3.80 (m, 1H), 4.04–4.11 (m, 1H), 4.60–4.69 (m, 1H), 6.87 (d, J = 8.0 Hz, 1H), 7.30–7.36 (m, 2H), 7.54 (d, J = 1.6 Hz), 7.93–7.98 (m, 2H), 11.30 (s, 1H); Compound **9** (DMSO-d_6): 2.15–2.25 (m, 1H), 3.05–3.23 (m, 3H), 3.27 (s, 3H), 3.73–3.80 (m, 1H), 3.83 (s, 3H), 4.02–4.10 (m, 1H), 4.60–4.69 (m, 1H), 6.85 (d, J = 8.0 Hz, 1H), 7.06 (dd, J = 8.8, 2.4 Hz, 1H), 7.29 (dd, J = 8.0, 2.0 Hz, 1H), 7.51 (d, J = 1.6 Hz, 1H), 7.62 (d, J = 2.4 Hz, 1H), 7.83 (d, J = 8.8 Hz, 1H), 11.30 (s, 1H); Compound **10** (DMSO-d_6): 2.14–2.28 (m, 1H), 2.84–2.95 (m, 1H), 2.98–3.05 (m, 1H), 3.17–3.27 (m, 1H), 3.61–3.71 (m, 1H), 3.86–4.00 (m, 2H), 4.38–4.46 (m, 1H), 7.00 (d, J = 8.0 Hz, 1H), 7.36–7.41 (m, 1H), 7.47–7.53 (m, 2H), 7.64 (d, J = 1.6 Hz, 1H), 7.98 (d, J = 8.0 Hz, 1H), 8.07 (d, J = 7.2 Hz, 1H), 9.46 (s, 1H); Compound **11** (DMSO-d_6): 2.15–2.23 (m, 1H), 2.83–2.94 (m, 1H), 2.97–3.05 (m, 1H), 3.18–3.28 (m, 1H), 3.60–3.71 (m, 1H), 3.86–4.01 (m, 2H), 4.36–4.46 (m, 1H), 6.99 (d, J = 8.0 Hz, 1H), 7.35 (td, J = 8.8, 2.4 Hz, 1H), 7.48 (dd, J = 8.0, 2.0 Hz, 1H), 7.57–7.64 (m, 1H), 7.96–8.02 (m, 2H), 9.46 (s, 1H); Compound **13** (DMSO-d_6): 2.15–2.27 (m, 1H), 2.85–2.95 (m, 1H), 2.96–3.04 (m, 1H), 3.18–3.27 (m, 1H), 3.64–3.74 (m, 1H), 3.91–4.00 (m, 2H), 4.47–4.57 (m, 1H), 7.12 (d, J = 8.0 Hz, 1H), 7.36–7.42 (m, 1H), 7.44–7.52 (m, 2H), 7.55 (d, J = 1.6 Hz, 1H), 7.98 (d, J = 7.6 Hz, 1H), 8.07 (d, J = 7.6 Hz, 1H), 9.47 (s, 1H); Compound **14** (DMSO-d_6): 2.15–2.27 (m, 1H), 2.85–2.95 (m, 1H), 2.96–3.04 (m, 1H), 3.18–3.29 (m, 1H), 3.63–3.74 (m, 1H), 3.91–4.00 (m, 2H), 4.46–4.55 (m, 1H), 7.12 (d, J = 8.4 Hz, 1H), 7.36 (td, J = 8.8, 2.4 Hz, 1H), 7.44 (dd, J = 8.0, 2.0 Hz, 1H), 7.53 (d, J = 2.0 Hz, 1H), 7.96–8.03 (m, 2H), 9.47 (s, 1H); Compound **15** (DMSO-d_6): 2.13–2.28 (m, 1H), 2.80–3.02 (m, 2H), 3.18–3.33 (m, 1H), 3.60–3.73 (m, 1H), 3.83 (s, 3H), 3.87–4.02 (m, 2H), 4.43–5.02 (m, 1H), 7.02–7.11 (m, 2H), 7.38 (dd, J = 8.1, 1.8 Hz, 1H), 7.49 (d, J = 1.8 Hz, 1H), 7.64 (d, J = 2.4 Hz, 1H), 7.85 (d, J = 8.7 Hz, 1H), 9.46 (s, 1H); Compound **16** (DMSO-d_6): 2.06–2.20 (m, 1H), 2.90–3.05 (m, 2H), 3.34–3.42 (m, 2H), 3.92–4.02 (m, 1H), 4.31–4.40 (m, 1H), 4.45–4.54 (m, 1H), 7.42–7.48 (m, 1H), 7.51–7.57 (m, 2H), 7.66–7.72 (m, 2H), 8.04 (d, J = 7.6 Hz, 1H), 8.12 (d, J = 7.6 Hz, 1H), 9.67 (s, 1H); Compound **17** (DMSO-d_6): 2.06–2.16 (m, 1H), 2.91–3.04 (m, 2H), 3.27–4.43 (m, 2H), 3.92–4.01 (m, 1H), 4.30–4.39 (m, 1H), 4.45–4.55 (m, 1H), 7.40 (td, J = 8.8, 2.4 Hz, 1H), 7.52 (dd, J = 8.0, 1.6 Hz, 1H), 7.65–7.70 (m, 2H), 8.02–8.08 (m, 2H), 9.69 (s, 1H); Compound **18** (DMSO-d_6): 2.02–2.18 (m, 1H), 2.90–3.05 (m, 2H), 3.85 (s, 3H), 3.88–4.03 (m, 2H), 4.28–4.53 (m, 2H), 7.12 (dd, J = 7.5, 2.1 Hz, 1H), 7.47 (d, J = 7.8 Hz, 1H), 7.55–7.75 (m, 3H), 7.92 (d, J = 8.7 Hz, 1H), 9.67 (s, 1H); Compound **19** (DMSO-d_6): 2.05–2.17 (m, 1H), 2.85–3.02 (m, 2H), 3.35–3.46 (m, 2H), 3.90–4.01 (m, 1H), 4.30–4.44 (m, 2H), 7.20 (d, J = 8.4, 1H), 7.37–7.53 (m, 2H), 7.79 (dd, J = 8.4, 2.0 Hz, 1H), 7.99 (d, J = 8.0 Hz, 1H), 8.09 (d, J = 7.6 Hz, 1H), 8.20 (d, J = 1.6 Hz, 1H), 9.66 (s, 1H); Compound **20** (DMSO-d_6): 2.06–2.19 (m, 1H), 2.86–3.01 (m, 2H), 3.35–3.48 (m, 2H), 3.91–4.00 (m, 1H), 4.31–4.44 (m, 2H), 7.20 (d, J = 8.8 Hz, 1H), 7.37 (td, J = 8.8, 2.4 Hz, 1H), 7.76 (dd, J = 8.4, 2.0 Hz, 1H), 7.97–8.04 (m, 2H), 8.18 (d, J = 1.6 Hz, 1H), 9.67 (s, 1H); Compound **22** ($CDCl_3$): 2.74–2.81 (m, 1H), 2.82 (s, 3H), 3.45–3.52 (m, 1H), 3.59–3.67 (m, 1H), 3.85–3.92 (m, 1H), 4.30–4.40 (m, 2H), 4.42–4.52 (m, 1H), 4.65–4.75 (m, 1H), 6.95 (d, J = 8.4 Hz, 1H), 7.49–7.56 (m, 2H), 7.63 (t, J = 8.0 Hz, 1H), 7.84 (d, J = 8.0 Hz, 1H), 8.50 (d, J = 8.4 Hz, 1H), 8.55 (s, 1H); Compound **23** ($CDCl_3$): 2.70–2.82 (m, 1H), 2.83 (s, 3H), 3.45–3.54 (m, 1H), 3.60–3.68 (m, 1H), 3.79–3.92 (m, 1H), 4.30–4.49 (m, 3H), 4.59–4.69 (m, 1H), 6.96 (d, J = 8.4 Hz, 1H), 7.36 (td, J = 8.8, 2.4 Hz, 1H), 7.49 (dd, J = 8.4, 2.4 Hz, 1H), 7.55 (dd, J = 7.6, 2.4 Hz, 1H), 8.36–8.46 (m, 2H); Compound **24** ($CDCl_3$): 2.60–2.72 (m, 1H), 2.79 (s, 3H), 3.40–3.52 (m, 1H), 3.63–3.75 (m, 1H), 3.80–3.88 (m, 1H), 3.91 (s, 3H), 4.23–4.41 (m, 2H), 4.43–4.61 (m, 2H), 6.97 (d, J = 8.1 Hz, 1H), 7.10 (dd, J = 8.0, 2.1 Hz, 1H), 7.32 (d, J = 2.1 Hz, 1H), 7.50 (d, J = 8.1 Hz, 1H), 7.80 (s, 1H), 8.02 (d, J = 8.7 Hz, 1H).
29. Klunk, W. E.; Wang, Y. M.; Huang, G. F.; Debnath, M. L.; Holt, D. P.; Mathis, C. A. *Life Sci.* **2001**, *69*, 1471.
30. Kim, M. K.; Choo, I. H.; Lee, H. S.; Woo, J. I.; Chong, Y. *Bull. Korean Chem. Soc.* **2007**, *28*, 1231.
31. Yang, Y.; Zhu, L.; Chen, X. J.; Zhang, H. B. *J. Mol. Graph. Model.* **2010**, *29*, 538.